Table 1 Fundamental frequency parameter $\omega ab(\rho/H)^{1/2}$ for a square orthotropic clamped plate subject to hydrostatic in-plane force (tension positive)

$D_x/H = D_y/H$		½		1		2	
$Na^2/\pi^2 H$		Bolotin	Series (Ref. 5)	Bolotin	Series (Ref. 5)	Bolotin	Series (Ref. 5)
−2	Conventional (Ref. 1)	15.784	17.742	26.726	28.573	40.900	42.641
	Modified	15.808		26.793		41.080	
0	Conventional (Ref. 1)	27.473	28.071	35.092	35.985	46.832	47.959
	Modified	27.476		35.112		46.915	
10	Conventional (Ref. 1)	54.927	54.981	59.802	59.925	67.913	69.165
	Modified	54.927		59.802		67.917	

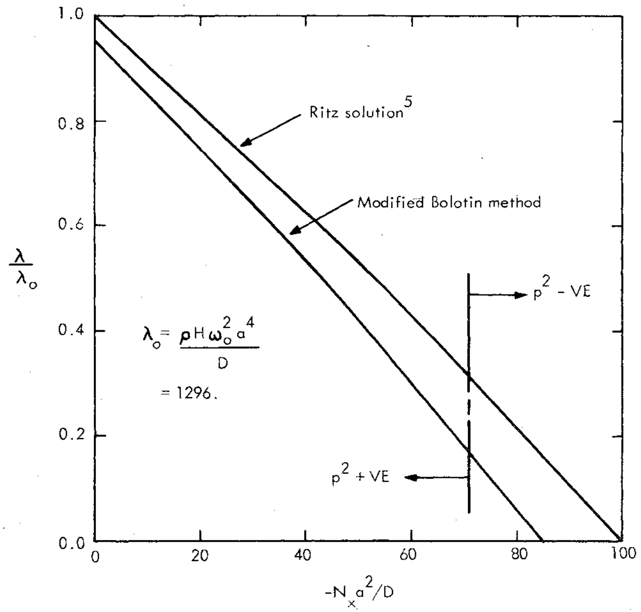

Fig. 1 Frequency parameter squared vs uniaxial in-plane force for square isotropic clamped plate.

plate under in-plane force N_x only, as computed using the modified Bolotin approach, and a Ritz approach.[6] Only the region in which N_x is compressive is shown to illustrate the performance of the modified Bolotin approach when γ_x [3,4] is imaginary, the region in which this occurs being indicated. As would be expected, there is no significant change in the nature of the curve as this region is entered.

It should be recognized that the performance of either Bolotin approach is relatively poor in the compressive in-plane force domain and that much more accurate results are obtained for tensile loadings.

References

[1] Dickinson, S.M., "Bolotin's Method Applied to the Buckling and Lateral Vibrations of Stressed Plates," *AIAA Journal*, Vol. 13, Jan. 1975, pp. 109-10.

[2] Bolotin, V.V., "An Asymptotic Method for the Study of the Problem of Eigenvalues for Rectangular Regions," *Problems of Continuum Mechanics (Volume Dedicated to N.I. Muskhelishvili), Society of Industrial and Applied Mathematics*, Philadelphia, Pa. 1961, pp. 56-68.

[3] Vijayakumar, K., "A New Method for Analysis of Flexural Vibration of Rectangular Orthotropic Plates," *Journal of the Aeronautical Society of India*, Vol. 23, 1971, pp. 197-204.

[4] Elishakoff, I.B., "Vibration Analysis of Clamped Square Orthotropic Plate," *AIAA Journal*, Vol. 12, July 1974, pp. 921-924.

[5] Dickinson, S.M., "The Flexural Vibration of Rectangular Orthotropic Plates Subject to In-plane Forces," *ASME Transactions: Journal of Applied Mechanics*, Vol. 38, Sept. 1971, pp. 699-700.

[6] Bassily, S.F. and Dickinson, S.M., "Buckling and Lateral Vibrations of Rectangular Plates Subject to In-plane Loads—A Ritz Approach," *Journal of Sound and Vibration*, Vol. 24, Sept. 1972, pp. 219-239.

Three-Dimensional Laminar Boundary Layer in Low-Speed Swirling Flow with Mass Transfer

Margaret Muthanna* and G. Nath†
Indian Institute of Science, Bangalore, India

SWIRLING flow occurs in rockets, jet engines, vortex valves, industrial furnaces, and many other types of machinery. In view of such a wide application of swirling flow, it is necessary to have a thorough understanding of such flows, if their design is to be accomplished on any kind of rational basis. Recently, Lewellen[1] and Murthy[2] made an extensive survey of swirling flows and their applications. The strong interaction that exists between the boundary layer and the outer flow in the case of rotating flows has been discussed by Rott and Lewellen.[3] The similarity solutions are quick and reliable solutions of these problems, which, if solved exactly, would require considerable manpower and computer time.

Back[4] has obtained the similarity solutions for low-speed three-dimensional laminar compressible boundary layer with swirl and without mass transfer on an axisymmetric surface of variable cross section. But, in his analysis, he employed the simplifying assumption that the density-viscosity product $\rho\mu$ is constant in the boundary layer and the Prandtl number Pr is unity.

Our objective in this study is to obtain similarity solutions of the above problem for a perfect gas, employing realistic gas properties ($\rho \propto H^{-1}$, $\mu \propto H^{\omega}$, $\mathrm{Pr} = 0.7$; where H and ω are the enthalpy and exponent of viscosity, respectively) together with mass transfer. We have clearly displayed the inadequacy of solutions obtained under the simplifying assumptions of $\omega = \mathrm{Pr} = 1$. We have used successfully the method of parametric differentiation in combination with quasilinearization to solve the governing equations.

Received May 7, 1975; revision received July 15, 1975.

Index category: Boundary Layers and Convective Heat Transfer-Laminar.

*Research Student, Department of Applied Mathematics.

†Associate Professor, Department of Applied Mathematics.

Governing Equations

The effect of swirl is investigated for low-speed flow of a perfect gas modeled realistically ($\rho \propto H^{-1}$, $\mu \propto H^{\omega}$, $\mathrm{Pr}=0.7$) with constant specific heat. The equations for laminar compressible boundary layer for low-speed swirling flow over an axisymmetric surface of variable cross section, caused by imposing a free vortex on longitudinal flow, under similarity assumptions, are[4]

$$(Cf'')' + ff'' + \bar{\beta}(g - f'^2) + \bar{\alpha}(g - s^2) = 0 \tag{1a}$$

$$(Cs')' + fs' = 0, \quad (Cg')' + \mathrm{Pr} fg' = 0 \tag{1b,c}$$

The boundary conditions are

$$\text{at } Z=0 \quad f=f_w \quad f'=0 \quad s=0 \quad g=g_w \tag{2a}$$

$$\text{at } Z\to\infty \quad f'\to 1 \quad s\to 1 \quad g\to 1 \tag{2b}$$

Here f is the dimensionless stream function; f', s, and g are the dimensionless longitudinal velocity, swirl velocity, and total enthalpy, respectively; $C=\rho\mu/\rho_e\mu_e=g^{\omega-1}$ is the density-viscosity ratio; $\bar{\alpha}$ and $\bar{\beta}$ are the swirl and longitudinal acceleration parameters respectively; g_w is the cooling parameter;

$$f_w = -\rho_w w_w (2X)^{1/2} / r\rho_e\mu_e u_e$$

is the dimensionless mass transfer parameter, $f_w>0$ for suction and $f_w<0$ for injection (w_w is the dimensional mass transfer parameter and other symbols like r and u_e are the same as in Ref. 4 except X, which corresponds to Ξ) and prime denotes differentiation with respect to the independent similarity variable Z.

We have neglected the viscous dissipation terms ($u_e^2/2H_{t_0}$, $v_e^2/2H_{t_0}$) in the governing equations since Gross and Dewey[5] have shown that they do not have any appreciable effect for low-temperature flows (i.e., $\omega=0.7$).

The skin-friction coefficient along the longitudinal direction C_f and the heat-transfer coefficient in the form of Stanton number St can be expressed as[4]

$$C_f = [2^{1/2} r\mu_e / X^{1/2}] C_w f''(0) \tag{3}$$

$$\mathrm{St} = [r\mu_e/(2X)^{1/2}] C_w g'(0)/\mathrm{Pr}(1-g_w) \tag{4}$$

Similarly, the surface shear stress along tangential direction τ_η is given by[4]

$$\tau_\eta = [v_e\rho_e u_e r\mu_e/(2X)^{1/2}] C_w s'(0) \tag{5}$$

Here $f''(0)$ and $s'(0)$ are the shear stress parameters in the longitudinal and tangential directions, respectively, $g'(0)$ is the heat-transfer parameter and η, v_e, and H_{t_0} are defined in Ref. 4.

Results

The Eqs. (1) for $\omega=\mathrm{Pr}=1$, together with the boundary conditions [Eqs. (2)] were first solved for various values of $\bar{\alpha}$, $\bar{\beta}$, f_w, and g_w by the method of quasilinearization.[4] Then employing these solutions as the starting values for the parameters ω and Pr, we have obtained the solutions of the governing Eqs. (1) under conditions of Eqs. (2) for various values of ω and Pr by the method of parametric differentiation.[6-8]

Tables 1-3 show the effect of $\bar{\alpha}$, $\bar{\beta}$, f_w, g_w and ω on shear stress and heat transfer parameters $f''(0)$, $s'(0)$, and $g'(0)$. The results reveal that, for fixed values of f_w, g_w, and ω, $f''(0)$, $s'(0)$, and $g'(0)$ increase as $\bar{\alpha}$ increases, for all values of $\bar{\beta}$. However, they decrease as $\bar{\beta}$ decreases for $\bar{\alpha}>0$, but when $\bar{\alpha}=0$, they increase with $\bar{\beta}$. Similarly, $f''(0)$, $s'(0)$ and $g'(0)$ decrease with ω, but the decrease is more pronounced when $g_w=0.2$, as compared to $g_w=0.6$. Also, $f''(0)$, $s'(0)$, and $g'(0)$ are increased due to suction, while injection does the reverse. When g_w is increased, $f''(0)$ and $s'(0)$ increase, but $g'(0)$ decreases. It may be mentioned that $f''(0)$ is strongly dependent on $\bar{\alpha}$ or g_w, whereas $g'(0)$ is weakly dependent on both parameters, but $s'(0)$ depends strongly on g_w but not on $\bar{\alpha}$. Again for large $\bar{\alpha}$, $s'(0)$ and $g'(0)$ are strongly dependent on f_w, whereas the dependence of $f''(0)$ on f_w is rather weak. It may be remarked that our results for $f_w=0$, $\omega=\mathrm{Pr}=1$ coincide with those obtained by Back[4] up to four decimal places.

Back[4] has suggested corrections to take into account the effect of $\omega\neq 1$, $\mathrm{Pr}\neq 1$ on the frictional coefficient C_f and Stanton number St. The suggested relations are[4]

$$C_f = (2^{1/2} r\mu_e/X^{1/2})\,(C_w)^{0.1}[f''(0)]_{\omega=\mathrm{Pr}=1} \tag{6}$$

$$St = [r\mu_e/(2X)^{1/2}]\,(C_w)^{0.1} \times [g'(0)]_{\omega=\mathrm{Pr}=1}/[\mathrm{Pr}^{2/3}(1-g_w)] \tag{7}$$

Table 1 Friction and heat-transfer parameters, $f''(0)$, $s'(0)$, $g'(0)$ for $\bar{\alpha}=0$, $\mathrm{Pr}=0.7$

$\bar{\beta}$	g_w	f_w	$\omega=0.7$			$\omega=1.0$		
			$f''(0)$	$s'(0)$	$g'(0)$	$f''(0)$	$s'(0)$	$g(0)$
0	0.2	-0.5	0.1283	0.1283	0.1136	0.1485	0.1485	0.1368
0	0.2	0	0.2988	0.2988	0.2129	0.4696	0.4696	0.3352
0	0.2	1.0	0.7426	0.7426	0.4539	1.2836	1.2836	0.7883
0	0.6	-0.5	0.1448	0.1448	0.0656	0.1485	0.1485	0.0684
0	0.6	0	0.4162	0.4162	0.1483	0.4696	0.4696	0.1676
0	0.6	1.0	1.1047	1.1047	0.3390	1.2836	1.2836	0.3942
1.0	0.2	-0.5	0.3432	0.1747	0.1441	0.4569	0.2266	0.1915
1.0	0.2	0	0.4908	0.3306	0.2320	0.7472	0.5159	0.3647
1.0	0.2	1.0	0.8819	0.7539	0.4602	1.4883	1.2986	0.7977
1.0	0.6	-0.5	0.6732	0.2476	0.1006	0.7271	0.2652	0.1089
1.0	0.6	0	0.9003	0.4853	0.1704	0.9991	0.5456	0.1921
1.0	0.6	1.0	1.4787	1.1310	0.3476	1.6919	1.3115	0.4034
5.0	0.2	-0.5	0.7069	0.2111	0.1844	0.9326	0.2767	0.2251
5.0	0.2	0	0.8161	0.3476	0.2472	1.2390	0.5591	0.3918
5.0	0.2	1.0	1.1822	0.7688	0.4573	1.9398	1.3218	0.8124
5.0	0.6	-0.5	1.5571	0.3098	0.1193	1.6896	0.3354	0.1322
5.0	0.6	0	1.7798	0.5438	0.1861	1.9594	0.6108	0.2128
5.0	0.6	1.0	2.3053	1.1685	0.3587	2.5928	1.3516	0.4164

Table 2 Friction and heat-transfer parameters, $f''(0)$, $s'(0)$, $g'(0)$ for $\bar{\alpha}=10$, Pr = 0.7

			$\omega=0.7$			$\omega=1.0$		
$\bar{\beta}$	g_w	f_w	$f''(0)$	$s'(0)$	$g'(0)$	$f''(0)$	$s'(0)$	$g'(0)$
0	0.2	-0.5	1.8940	0.3535	0.2599	2.7208	0.5082	0.3843
0	0.2	0	2.0166	0.4893	0.3307	3.0357	0.7619	0.5260
0	0.2	1.0	2.1887	0.8443	0.5143	3.4559	1.4266	0.8809
0	0.6	-0.5	4.2050	0.5597	0.2067	4.6058	0.6147	0.2289
0	0.6	0	4.4605	0.7735	0.2658	4.9294	0.8677	0.2994
0	0.6	1.0	4.7438	1.3140	0.4091	5.2971	1.5112	0.4711
1.0	0.2	-0.5	1.6325	0.3143	0.2295	2.3145	0.4493	0.3429
1.0	0.2	0	1.7755	0.4546	0.3322	2.6633	0.7130	0.4926
1.0	0.2	1.0	2.0399	0.8279	0.4998	3.2378	1.4054	0.8667
1.0	0.6	-0.5	3.7273	0.5020	0.1861	4.0651	0.5487	0.2055
1.0	0.6	0	4.0113	0.7234	0.2480	4.4167	0.8104	0.2794
1.0	0.6	1.0	4.4357	1.2864	0.3991	4.9452	1.4804	0.4601
5.0	0.2	-0.5	1.4875	0.2783	0.2154	2.0573	0.3839	0.2971
5.0	0.2	0	1.5474	0.3109	0.3038	2.4072	0.6576	0.4550
5.0	0.2	1.0	1.8326	0.7612	0.4140	3.0948	1.3807	0.8501
5.0	0.6	-0.5	3.5126	0.4309	0.1546	3.8268	0.4732	0.1768
5.0	0.6	0	3.7835	0.6620	0.2196	4.1588	0.7432	0.2559
5.0	0.6	1.0	4.2936	1.2524	0.3844	4.7771	1.4434	0.4468

Table 3 Friction and heat-transfer parameters, $f''(0)$, $s'(0)$, $g'(0)$ for $\bar{\alpha}=20$, Pr = 0.7

			$\omega=0.7$			$\omega=1.0$		
$\bar{\beta}$	g_w	f_w	$f''(0)$	$s'(0)$	$g'(0)$	$f''(0)$	$s'(0)$	$g'(0)$
0	0.2	-0.5	3.0986	0.4279	0.3069	4.5004	0.6259	0.4641
0	0.2	0	3.2222	0.5616	0.3748	4.8554	0.8769	0.6020
0	0.2	1.0	3.3389	0.9016	0.5482	5.2075	1.5126	0.9378
0	0.6	-0.5	7.0058	0.6873	0.2498	7.6849	0.7573	0.2775
0	0.6	0	7.2974	0.8999	0.3078	8.0603	1.0091	0.3468
0	0.6	1.0	7.5370	1.4203	0.4449	8.3894	1.6288	0.5111
1.0	0.2	-0.5	2.5885	0.3706	0.2581	3.7355	0.5500	0.4110
1.0	0.2	0	2.7296	0.5046	0.3723	4.1425	0.8111	0.5571
1.0	0.2	1.0	2.9905	0.8726	0.5209	4.7095	1.4770	0.9137
1.0	0.6	-0.5	6.0441	0.6124	0.2231	6.6017	0.6720	0.2473
1.0	0.6	0	6.3821	0.8329	0.2841	7.0236	0.9327	0.3201
1.0	0.6	1.0	6.9181	1.3712	0.4199	7.6012	1.5581	0.4901
5.0	0.2	-0.5	2.1765	0.3227	0.2449	3.0095	0.4509	0.3421
5.0	0.2	0	2.3460	0.4681	0.3218	3.4099	0.7224	0.4971
5.0	0.2	1.0	2.4641	0.7692	0.4029	4.1245	1.4265	0.8797
5.0	0.6	-0.5	5.1531	0.5032	0.1746	5.6236	0.5571	0.2067
5.0	0.6	0	5.4637	0.7183	0.2300	6.0122	0.8264	0.2833
5.0	0.6	1.0	6.0177	1.3126	0.4030	6.6741	1.5094	0.4688

The present results for C_f and St with or without swirl ($\bar{\alpha} \geqslant 0$) and without mass transfer ($f_w = 0$) for $\omega = \mathrm{Pr} = 0.7$ have been compared with the corresponding results obtained from Eqs. 6 and 7. It has been found that they are in good agreement, the maximum difference being about 5%. Hence, it can be concluded that the suggested corrections are valid both for swirling and nonswirling flows.

It was observed that there is a velocity overshoot in the longitudinal velocity f' (profiles are not shown graphically for the sake of brevity) for $\bar{\alpha} > 0$, $\bar{\beta} \geqslant 0$, $\omega = 1.0$ and 0.7, and $f_w \leqslant 0$. The *reasons* for the occurrence of a velocity overshoot is given by Back.[4] The velocity overshoot increases as $\bar{\alpha}$ or ω increases, but it decreases as $\bar{\beta}$ or f_w ($f_w \leqslant 0$) increases. It may be remarked that similar effects have been observed by Back[4] for $\omega = 1$ and for no mass transfer. Another important feature observed is that the s and g profiles have a point of inflection for $\omega = 0.7$, whatever may be the value of $\bar{\alpha}$, $\bar{\beta}$, f_w and g_w as is evidenced by a maximum in s' and g' (profiles for s' and g' are not shown graphically for lack of space). However, when $\omega = 1$, s and g have a point of inflection only for injection ($f_w < 0$). Gross and Dewey,[5] and Vimala and Nath[7] have observed similar effects on using the power-law variation for viscosity ($\omega \neq 1$) for two- and three-dimensional stagnation-point flows.

Conclusions

It can be concluded that the effect of the variation of the density-viscosity product ratio ($\omega \neq 1$) across the boundary-layer on shear stress and heat-transfer parameters is appreciable only at low wall temperature, which indicates that the linear viscosity-temperature relation ($\omega = 1$) does not hold good for low wall temperature. Also, this variation gives rise to a point of inflection in swirl velocity and total enthalpy profiles. However, for injection, swirl velocity and total enthalpy profiles have a point of inflection even when the density-viscosity product is constant.

References

[1] Lewellen, W. S., "A Review of Confined Vortex Flows," NASA CR-1772, 1971.

[2] Murthy, S. N. B., "Survey of Some Aspects of Swirling Flows," USAF, ARL 71-0244, 1971.

[3] Rott, N. and Lewellen, W. S., "Boundary Layers and Their Interactions in Rotating Flows," *Progress in Aeronautical Science*, Vol. 7, Pergamon Press, Oxford, 1966, pp. 111-144.

[4] Back, L. H., "Flow and Heat Transfer in Laminar Boundary Layers with Swirl," *AIAA Journal*, Vol. 7, Sept. 1969, pp. 1781-1789.

[5] Gross, J. F. and Dewey, C. F., "Similar Solutions of the Laminar Boundary-Layer Equations with Variable Fluid Properties," *Fluid Dynamics Transactions*, Vol. 2, Pergamon Press, Oxford, 1965, pp. 529-548.

[6] Rubbert, P. E., "Analysis of Transonic Flow by Means of Parametric Differentiation," Ph. D. Dissertation, 1965, Dept. of Mech. Eng., MIT, Cambridge, Mass.

[7] Vimala, C. S. and Nath, G., "Heat and Mass Transfer at a General Three-Dimensional Stagnation Point," *AIAA Journal*, Vol. 13, June 1975, pp. 711-712.

[8]Na. T. Y. and Turski, C. E., "Solution of the Non-Linear Differential Equations for Finite Bending of a Thin-Walled Tube by Parametric Differentiation," *Aeronautical Quarterly*, Vol. 25, Part 1, Feb. 1974, pp. 14-18.

Flow-Establishment Times for Blunt Bodies in an Expansion Tube

Charles G. Miller* and John A. Moore*
NASA Langley Research Center, Hampton, Va.

Nomenclature

M = Mach number
p_s = model surface pressure, kN/m^2
$\dot{q}_s$ = model surface heat transfer rate, MW/m^2
r_b = model base radius, cm
r_n = sphere nose radius, cm
t = time after arrival of incident shock in acceleration gas, μs
t^* = time required for shock standoff distance to obtain a steady-state value, μs
δ = shock standoff distance as function of time, cm
Δ = steady-state shock standoff distance, cm
ϵ = normal shock density ratio
τ = time interval between incident shock in acceleration gas and the interface, μs

Subscripts
5 = test gas freestream conditions
20 = acceleration gas freestream conditions

Introduction

DUE to the relatively short test-flow duration of the Langley expansion tube (approximately 100-300 μs), the time required to establish quasi-steady flow about a test model is an important consideration in data analysis. The expansion tube operating sequence differs from other hypersonic-hypervelocity impulse facilities since the test model is subjected to the acceleration gas flow prior to the test gas flow. Although results from studies of flow establishment times for blunt bodies in shock tubes (see Refs. 1-5) provide a guide, they are not directly applicable to the expansion tube. The purpose of this Note is to present flow establishment results as inferred from shock standoff distance, pressure, and heat transfer measurements in the Langley expansion tube. These experimental results were obtained as spinoff from various studies using helium, air, and CO_2 test gases at freestream velocities from 5-7 km/sec, and are preliminary to a more comprehensive study.

Apparatus and Tests

The expansion tube is basically a shock tube with a section of constant-cross-section tube attached to the downstream end. A weak, low-pressure (secondary) diaphragm separates this section, denoted as the acceleration section, from the driven section of the shock tube, which is commonly referred to as the intermediate section of the expansion tube. The intermediate section and acceleration section are evacuated and filled with the desired test gas and acceleration gas, respectively. For a given test, the acceleration gas was the same as the test gas, only at a much lower quiescent pressure. Upon rupture of the primary diaphragm in the shock-tube portion of the facility, the quiescent test gas is processed by the resulting incident shock wave. This shock-heated test-gas flow encounters and ruptures the secondary diaphragm, thereby generating an incident shock in the quiescent acceleration gas. The test gas undergoes an unsteady expansion in the acceleration section; hence, a model positioned at the exit of the acceleration section is subjected first to the incident shock in the acceleration gas and then to the shock-heated acceleration gas prior to the test gas flow. A more detailed description of the Langley 6-in.-diam expansion tube in presented in Ref. 6, along with the test-section flow conditions for the three test gases used in this study.

Shock standoff distance, δ was obtained using a single-pass Z-shaped schlieren system. Two recording systems were used simultaneously. One used a Xenon arc lamp as a light source and a high-speed framing camera to record the images. Camera speeds for the present study provided nominal time intervals between successive frames of 6.9 or 10.4 μs. This system was alined slightly off-axis and mirrors were used to prevent interference with the other system. The second system used a point light source, having a duration of approximately 150 *ns*, in conjunction with a still camera. The spark source for the still camera was alined on axis to yield the accuracy required for shock shape measurements.[6]

Model surface pressure p_s was measured using miniature piezoelectric (quartz) transducers in conjunction with charge amplifiers. These transducers were exposed to the model surface through a hole having a 1.6 mm diam and drilled at any angle so as to shield the sensing surface of the transducer from solid contaminants in the post-test flow.

Model-surface heat-transfer rates $\dot{q}_s$ were obtained using thin-film resistance gages having Pyrex 7740 substrates, platinum sensing elements, and silicone monoxide insulating films. These gages were mounted flush with the model surface and in the stagnation region. Convective heat transfer rate was determined using the voltage change of the sensing element during the test period as input to the computational method of Ref. 7.

Models tested were flat-faced cylinders and a sphere. The radius of the flat-faced cylinders r_b was varied from 0.95-3.81 cm, and the radius of the sphere r_n was 3.18 cm. Models were positioned at the acceleration section exit and tested in the open jet at zero angle of attack.

Results and Discussion

Measured normalized shock standoff distance for flat-faced cylinders of various radii and a sphere are shown in Fig. 1 as a function of test time t. Test gases are air (Fig. 1 a) and CO_2 (FIG. 1 b) at freestream Mach numbers, M_5 of 7.7 and 9.2, and normal shock density ratios, ϵ of 11.1 and 18.8, respectively. Establishing a zero time t from the film strip was not possible; hence, the first frame indicating flow about the model was assumed to correspond to a time equal to half the time interval between successive frames. Poor shock resolution of enlargements of each film frame and off-axis alinement prohibit accurate determination of shock standoff distance δ; however, the time history of δ is believed to be reasonably accurate. For a given test, values of δ for the flat-faced cylinder models were adjusted (up to 25%) to improve agreement between these values at times corresponding to essentially constant δ with the quasi-steady shock standoff distance, Δ obtained with the still camera at time t equal to 140-180 μs. Also shown in Fig. 1 are predicted[8,9] Δ for the acceleration gas flow and test gas flow. The time interval between arrival of the incident shock and the interface was inferred previously[6] to be 25-30 μs for air and CO_2.

The flat-faced cylinder results for air show a monotonic increase in δ/r_b to an essentially constant value for the three smaller radii; for the largest radius, δ/r_b initially increases, then decreases and finally increases to a nearly constant value. Similar trends are observed for CO_2. Thus, an effect of r_b on the variation of δ/r_b with t exists for the present air and CO_2 conditions. For air, the shock established symmetrically about

Received May 23, 1975; revision received July 14, 1975.
Index categories: Nonsteady Aerodynamics; Supersonic and Hypersonic Flow.

*Aero-Space Engineer, Entry Gas Dynamics Group, Advanced Entry Analysis Branch, Space Systems Division. Member AIAA.